

Directional smoothing of non-stationary filters

Robert G. Clapp, Sergey Fomel, Sean Crawley, and Jon F. Claerbout¹

keywords: helix, non-stationary, filtering, steering

ABSTRACT

Space-varying prediction error filters are an effective tool in solving a number of common geophysical problems. To estimate these filters some type of regularization is necessary. An effective method is to smooth the filters along radial lines in CMP gathers where dip information is relatively unchanging.

INTRODUCTION

Estimating filters is routine in seismic processing. The simplest example might be deconvolution, but filter estimation is also valuable in many other aspects of seismic processing: interpolation (Spitz, 1991; Crawley, 1998), noise attenuation (Canales, 1984; Soubaras, 1994; Abma, 1995), missing data (Claerbout, 1998; Fomel et al., 1997), and coherency estimation (Schwab, 1998; Bednar, 1997) to name just a few. All of these processes are based on the concept of finding a filter that minimize the energy when it is applied to a given set of data. The fundamental assumption is that that statistics of the data does not change spatially. This is often not the case. One solution to this problem is to separate the data into a number of overlapping patches (Claerbout, 1992d) where the stationary statistic assumption is more valid. Unfortunately, there is a limit to how small we can make our patches and still gather sufficient statistics.

A way around this limitation is to estimate a space varying prediction error filter (PEF) (Crawley et al., 1998). In the extreme case you can think of estimating a filter at every data location, or more realistically, at a coarser grid spacing. With so many filters and, as result, so many filter coefficients, our estimation can quickly turn into an undetermined or at least poorly determined problem. Therefore we must impose some type of regularization to our estimation problem. Choosing an appropriate regularization then becomes an issue. In this paper we argue that when estimating filters on seismic CMP data, you should smooth along radial lines. In a constant velocity medium the dip along a radial trace does not change, but in a more complex media it will vary slowly (Ottolini, 1982). By limiting filter variation in the radial direction we gather more data in our filter estimation thus enhancing stability. Here we show how to estimate the appropriate smoothing direction, and how to build and

¹email: bob@sep.Stanford.EDU, sean@sep.Stanford.EDU, sergey@sep.Stanford.EDU, jon@sep.stanford.edu

apply the appropriate regularization.

WHY SMOOTH RADIALLY

Dips change quickly along every axis in seismic data. As a result a single PEF has trouble characterizing it, even in small patches (Crawley, 1999). By estimating a space-varying PEF, we can overcome this deficiency. Unfortunately, this changes our estimation problem from something overdetermined to something, at times, grossly underdetermined. To stabilize our filter estimation we must apply some type of regularization to the standard PEF estimation optimization goals:

$$\begin{aligned} \mathbf{0} &\approx \mathbf{Y}\mathbf{a} \\ \mathbf{0} &\approx \epsilon\mathbf{F}\mathbf{a} \end{aligned} \quad (1)$$

where \mathbf{a} is our space-varying filter, \mathbf{Y} is convolution with our data, and \mathbf{F} is a roughener. To speed up convergence, we can take advantage of helix theory (Claerbout, 1998b) and reformulate our regularized problem into a preconditioned one

$$\begin{aligned} \mathbf{0} &\approx \mathbf{Y}\mathbf{F}^{-1}\mathbf{A}^{-1}\mathbf{p} \\ \mathbf{0} &\approx \epsilon\mathbf{p} \end{aligned} \quad (2)$$

where

$$\mathbf{p} = \mathbf{F}\mathbf{a}. \quad (3)$$

Our choice for \mathbf{F} can have significant influence on both the speed and quality of our filter estimation. The character of seismic data itself gives us a clue on what type of regularization we should use. A PEF filter is most successful when the statistics of the data it is being estimated from are stationary. Logically, our rougher \mathbf{F} , or \mathbf{F}^{-1} , should tend to smooth along a region with consistent dips, or along Snell traces (Claerbout, 1978). Figure 1 shows several constant velocity hyperbolas, with the same dips highlighted. These dips all fall along a radial line through zero time and zero offset. If we look at hyperbolas in $v(z)$, Figure 2, we see that there is deviation from a simple line, but generally this trend is preserved.

CHOOSING SMOOTHING DIRECTIONS

Prediction-error filters work best on predicting local plane waves (Claerbout, 1992c; Canales, 1984). With non-stationary filters, it is possible to predict data with variable slopes. For preconditioning the filter estimation problem, such filters can be smoothed along the direction where the slope stays locally constant. To put this principle into a mathematical form, let us denote the monodop data as $P(x, y)$, where x and y are the coordinate values. On a seismic data section, the y coordinate would have the meaning of time, but here we would

Figure 1: Constant velocity curves. The thick lines are the same dip on all the reflectors. Note how they form a line. `bob3-dips.constant` [ER]

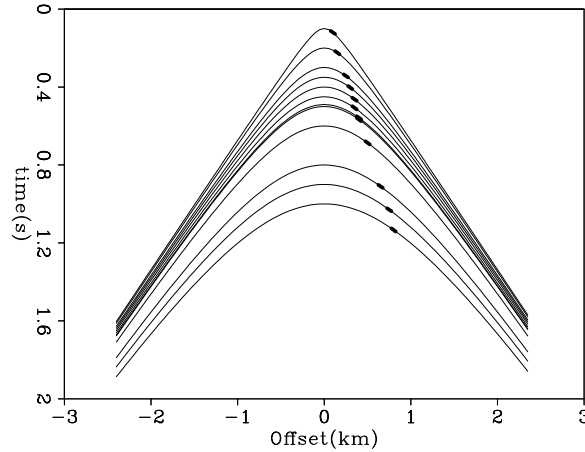
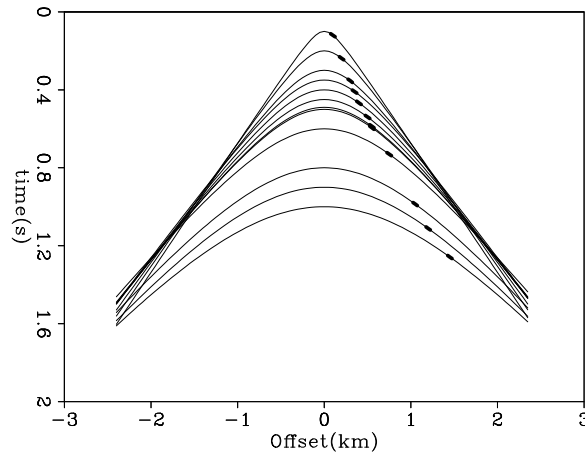


Figure 2: $V(z)$ medium curves. The thick lines represent the same dip. Note how they are not perfectly linear but generally lay along a line. `bob3-dips.vz` [ER]



like to develop a general method that would work on different kinds of data. The local dip field of the data can be defined by the formula

$$D(x, y) = -\frac{P_x}{P_y}, \quad (4)$$

where P_x and P_y denote the first partial derivatives: $P_x = \frac{\partial P}{\partial x}$, $P_y = \frac{\partial P}{\partial y}$. To validate formula (4), consider a plane-wave model with the slope s :

$$P(x, y) = P_0(y - sx). \quad (5)$$

Substituting (5) into formula (4), we can see that the $D(x, y)$ indeed produces an estimate of s (Claerbout, 1992). In the general case, $D(x, y)$ corresponds to the tangent of the local plane wave angle, measured from the x axis in the direction of the y axis. Bednar (1997) describes an application of formula (4) for computing coherency attributes. Instead of using formula (4) explicitly, we intend to estimate prediction-error filters that would destroy local plane waves in the data (Claerbout, 1992c; Schwab, 1998). To precondition the filter estimation problem we can smooth the filters in the direction of the least change in the slope. By analogy with (4), the smoothing direction can be defined as follows:

$$S(x, y) = -\frac{D_x}{D_y}, \quad (6)$$

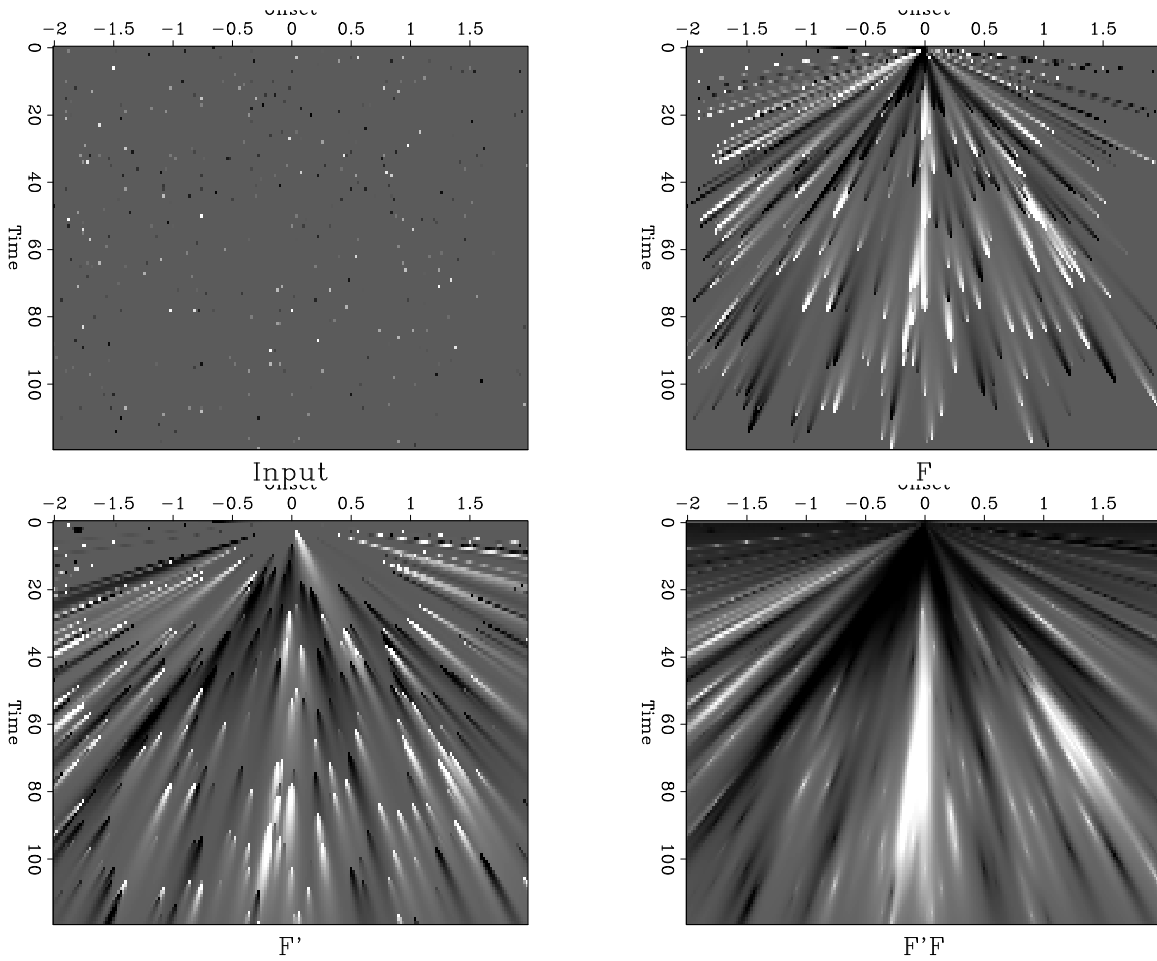


Figure 3: The effect of dip smoothing. The top-left panel is the input, the top-right is the result of applying the forward operator, bottom-left is the adjoint response; and bottom-right is the cascade of forward and the adjoint. `bob3-random` [ER]

or, substituting formula (4),

$$S(x, y) = -\frac{P_x P_{xy} - P_y P_{xx}}{P_y P_{xy} - P_x P_{yy}}, \tag{7}$$

where P_{xx} , P_{yy} , and P_{xy} are the corresponding second-order partial derivatives. An important analytical test case is a constant-velocity CMP gather, composed of reflection hyperbolas:

$$P_{\text{hyper}}(x, y) = P_0 \left(\sqrt{y^2 - s^2 x^2} \right). \tag{8}$$

Substituting (8) into formula (7) leads to the expression

$$S_{\text{hyper}}(x, y) = \frac{y}{x}, \tag{9}$$

which suggests smoothing the estimated prediction-error filters along radial lines on the $\{x, y\}$ plane (Crawley et al., 1998). Figure 4 and 5 illustrate a practical application of

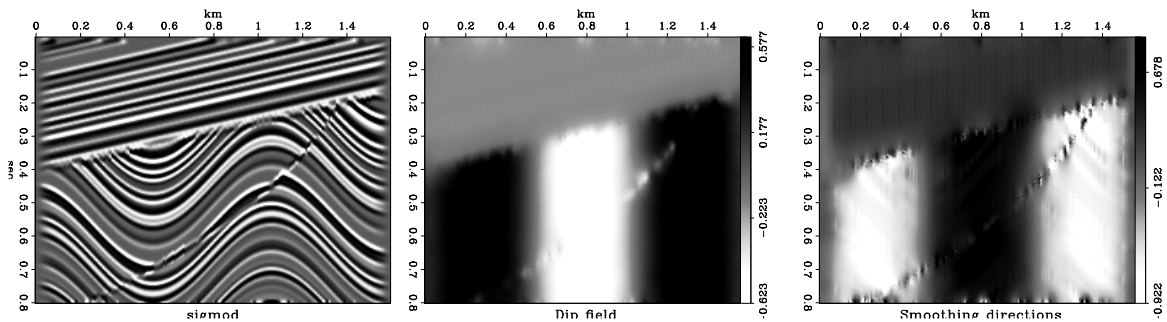


Figure 4: Synthetic model from *Basic Earth Imaging* (left), its estimated dip field (center), and estimated smoothing directions (right). `bob3-sigmod` [ER]

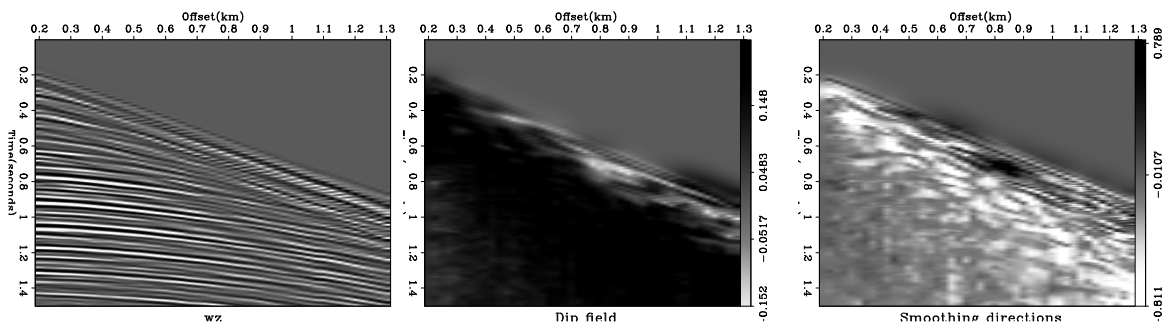


Figure 5: Seismic shot gather (left), its estimated dip field (center), and estimated smoothing directions (right). `bob3-wz` [ER]

formulas (4) and (6) on a synthetic reflectivity model from *Basic Earth Imaging* (Claerbout, 1995) and on a shot gather from the Yilmaz collection (Yilmaz, 1987). In both cases the first- and second-derivative operators were computed with simple finite-difference schemes.

To avoid a non-stable division in formulas (4) and (6), we solve the regularized least-square system

$$\begin{cases} \mathbf{D}\mathbf{x} \approx \mathbf{N} \\ \epsilon \nabla \mathbf{x} \approx \mathbf{0} \end{cases}, \quad (10)$$

where \mathbf{D} and \mathbf{N} denote the denominator and the numerator respectively, ϵ is the scalar regularization parameter, and \mathbf{x} is the estimated regularized ratio. Our simple two-point finite-difference scheme does not handle correctly the aliased dips on the seismic gather in Figure 5. Nevertheless it produces a reasonable output, which we can use as a rough estimate of the smoothing directions.

HOW TO SMOOTH RADIALLY

Once we know what directions we wish to smooth in, we must build an operator that can smooth in the desired directions. We want to minimize the cost of smoothing, so we would like the filters to be small. As discussed in Clapp (1997) an effective method is to build a series of small plane-wave annihilation filters (Claerbout, 1992b) and then combine them into a single operator.

Constructing a filter

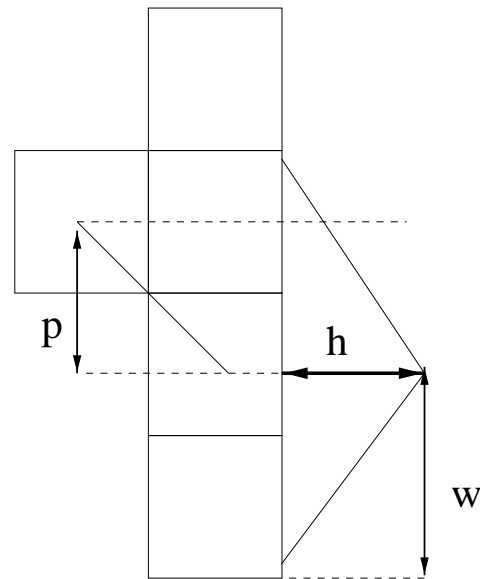
The basic idea in building a steering filter is to create a filter that destroys a given slope p . Further, we would like to keep differences of the bandwidth response for filters oriented at different slopes to a minimum. We can achieve both these goals by constructing a triangle centered at the appropriate slope (Figure 6.) Every grid cell center which the triangle passes through is assigned a negative value proportional to the height of the triangle at that location. The wider the triangle base, the less precise, and more Gaussian-like our smoother becomes, Figure 7. By decreasing the sum of the coefficients (with a hard limit of -1 to ensure filter stability when applying polynomial division (Claerbout, 1976)), we can spread information larger distances.

Control

The number of adjustable parameters in the filter construction is both a curse and a blessing. Whenever you add parameters to your problem, the model space that you have to search increases exponentially. With two adjustable parameters, taken to the extreme, at every model point, the task can seem daunting. Generally, the smartest course is to keep these two parameters constant throughout the whole model space. But, this freedom also opens up interesting possibilities. In certain regions of the data you might feel that the radial assumption is not quite valid, or that dips aren't changing quite as fast. In this region you could consider making your triangle bigger, smoothing your filter coefficients over a wider angle range, while keeping it small in areas where dip changes quickly. The sum of the non-zero lag coefficients opens up another intriguing freedom. As Figure 8 shows, when

Figure 6: A finite-difference star for a monoplane rejection filter. The left column contains a '1'. The right column contains samples off a triangle. The desired slope is represented by p , the smaller w the more precise the dip smoothed, and the larger h the bigger the area the smoother acts on.

`bob3-steering` [NR]



the sum of the non-zero lag coefficients gets close to -1 , the area over which the smoother operates increases greatly. This is similar to increasing the ϵ value over only a portion of your model space. This gives you the freedom to easily smooth regions where filter stability is questionable, while allowing high frequency changes in areas of good data.

Applying filter

As discussed by Claerbout (1998), by defining our filters in helix space we can use polynomial division to apply their inverse. This same principal holds true for space varying filters. The basic algorithm is:

```
integer function npolydiv(adj,add,model,data){
logical                :: adj,add
real                  :: xx(:),yy(:)
integer               :: ia, ix, iy, ip
integer, dimension(:), pointer :: lag
real,   dimension(:), pointer :: flt,tt
allocate(tt(size(yy)))
tt = 0.
if( adj) {
    tt = yy
    do iy= nd, 1, -1 { ip = aa%pch( iy)
        lag => aa%hlx( ip)%lag; flt => aa%hlx( ip)%flt
        do ia = 1, size( lag) {
            ix = iy - lag( ia);    if( ix < 1) cycle
            tt( ix) -= flt( ia) * tt( iy)
        }
    }
    xx += tt
} else {
```

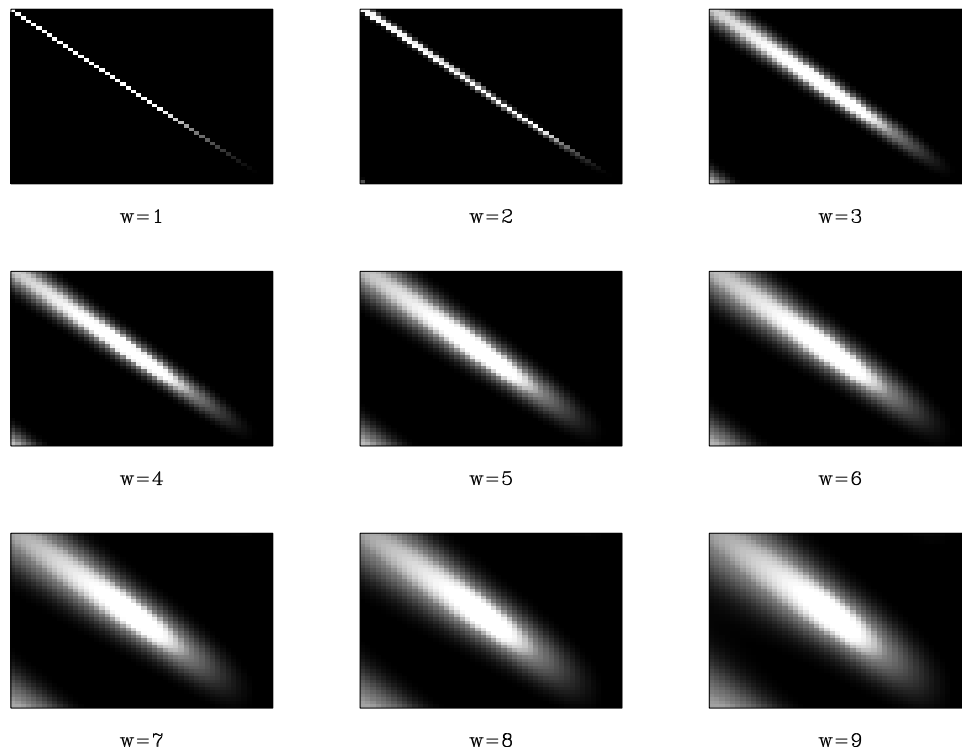



Figure 7: The impulse response of the smoothing filter as function of the triangle base. Note the wider the base, the less precise the dip smoothing. `bob3-width` [ER]

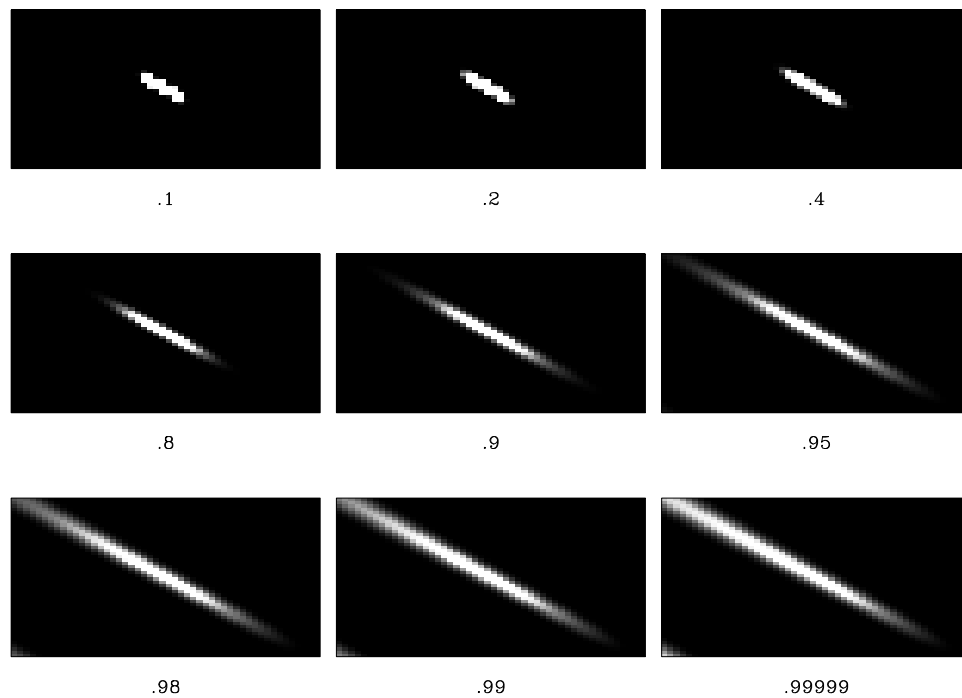


Figure 8: The impulse response of the smoothing filter as the sum of the non-zero lag coefficients get closer to 1. `bob3-distance` [ER]

```

    tt = xx
do iy= 1, nd { ip = aa%pch( iy)
  lag => aa%hlx( ip)%lag; flt => aa%hlx( ip)%flt
  do ia = 1, size( lag) {
    ix = iy - lag( ia);      if( ix < 1) cycle
    tt( iy) -= flt( ia) * tt( ix)
  }
}
yy += tt
}
allocate(tt(size(yy)))
}

```

PREDICTING A CMP GATHER

To show how radial smoothing can be valuable, we constructed a synthetic CMP gather using a Kirchhoff modeling code. To these CMP gathers we added two lines, one in a radial direction and one at constant time (left panel of Figure 9.) The constant time line can be thought of as noise, while the radial line represents conflicting information that fits our model of valid data. We then attempted to estimate the shot gather using fitting goals (3) with filters every 20 points in time and every 5 points in offset using two different types of preconditioners. The center panel shows the residual after using an inverse Laplacian (Claerbout, 1998b) and the right panel, radial smoothers. Generally, the two approaches did approximately the same job in predicting the data. The difference comes where the lines intersect the hyperbolas. If we examine the intersection points, more closely, Figure 10, we see that in the case of the Laplacian we did an equal job of predicting the hyperbolas and the constant time line. When using steering filters, the constant time line is much stronger (we avoid predicting noise).

INTERPOLATING A CMP GATHER

Once filters are estimated, one of their potential uses is missing data interpolation. Systematic gaps in data acquisition may cause data aliasing sufficient to make some processing steps difficult (Spitz, 1991; Crawley, 1998). Adding more traces can dealias the data. To add more traces, we require that the original data and the new data have the same dips (Claerbout, 1997). The dip information is carried in the PEFs. The missing data estimation is formulated just like the filter estimation, except that the PEFs are known and the data unknown. Also, we constrain the data by specifying that the originally recorded traces do not change. To separate the known and unknown data we have a known data selector \mathbf{K} and an unknown data selector \mathbf{U} , with $\mathbf{U} + \mathbf{K} = \mathbf{I}$. These multiply by 1 or 0 depending on whether the data was originally recorded or not. With \mathbf{A} signaling convolution with the PEF and \mathbf{y} the vector of data, the regression is $0 \approx \mathbf{A}(\mathbf{U} + \mathbf{K})\mathbf{y}$, or $\mathbf{A}\mathbf{U}\mathbf{y} \approx -\mathbf{A}\mathbf{K}\mathbf{y}$. Filters at

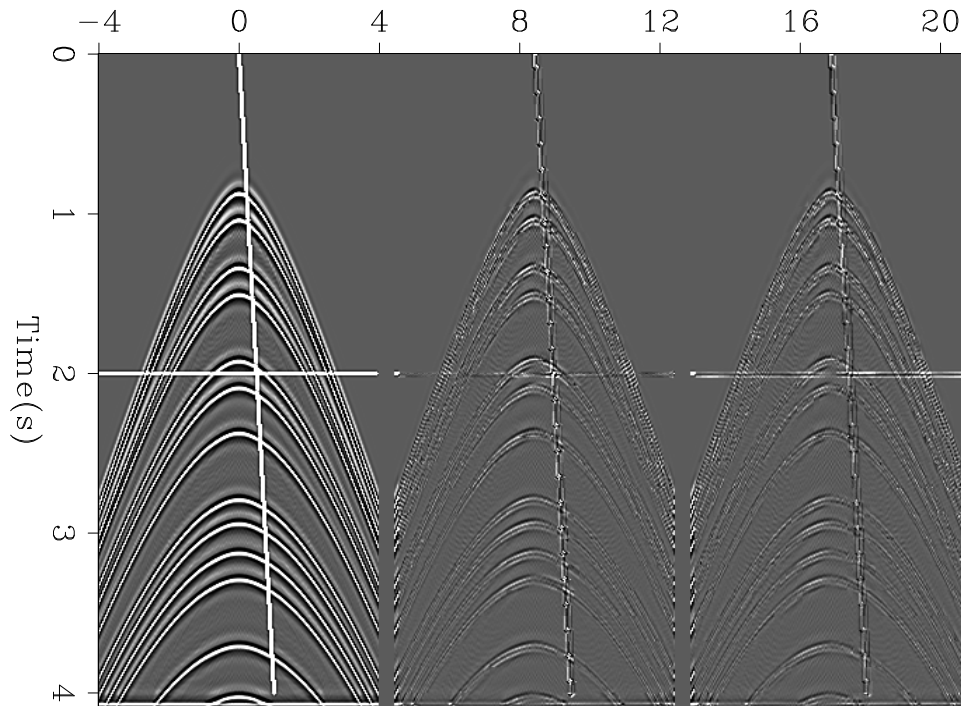


Figure 9: The result after 15 conjugate gradient steps of fitting goals (3). The left panel is the input, the center is using an inverse Laplacian preconditioner, the right panel is using radial smoothing. `bob3-comparison1` [ER]

every data point are cumbersome to estimate, so we estimate filters over small areas. This is just like patching (Claerbout, 1992d) except that now the patches are not independent. If the patches are independent, there is a lower limit on the patch size, because a patch must contain plenty of data to provide enough fitting equations to determine all the filter coefficients. Experience shows that where the data have curvature, the minimum patch size tends to be too large for the assumption of stationarity to be reasonable. Smoothing the filters allows us to make the patches much smaller, so that stationarity assumptions are workable. We arrange the new patches in polar coordinates, to take advantage of the notion of radial smoothing. An illustration is given in Figure 11. The cmp gather is overlaid by lines which delineate patch boundaries. Degree of smoothing in r and θ is adjustable. The patches shown are fairly large. Crawley and Claerbout(1999) explains further this method and shows the result of interpolating using radial patches and smoothers.

CONCLUSIONS

As the progress report deadline arrived, the authors were uncertain among themselves whether the results were correct. The prediction-error filters have clearly reduced the output variance, but the results do not clearly show the dip dependences that we expected. Generally we expected to see strong energy locally where events cross, and we expected to see

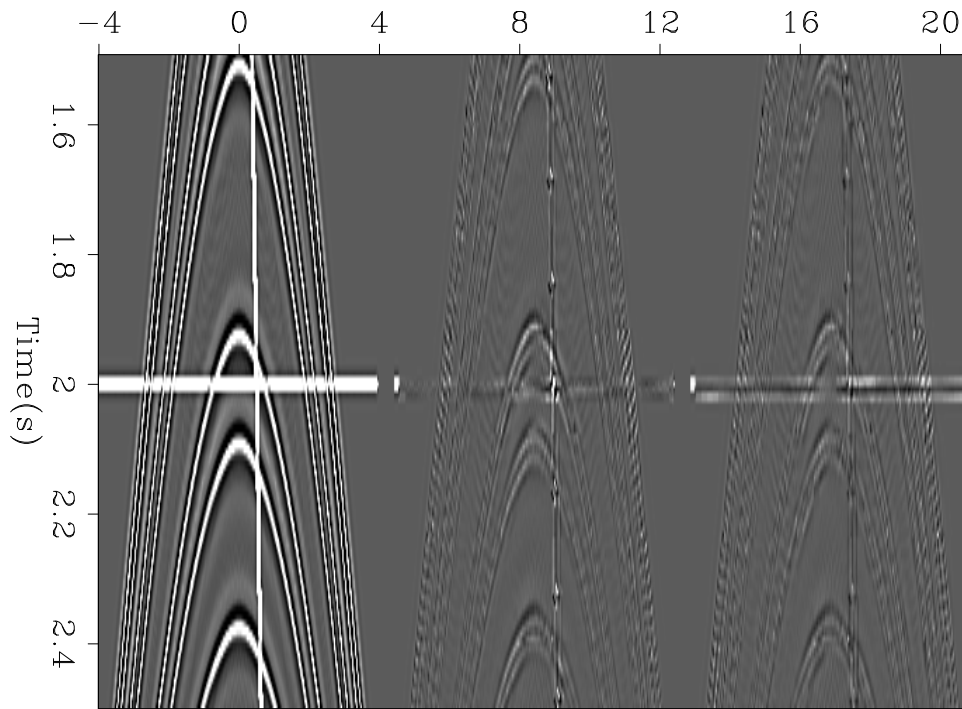


Figure 10: An enlargement of Figure 9. Note that the constant time line, what we consider noise, is much better predicted by the inverse Laplacian (center panel) than by radial smoothing. [bob3-comparison2](#) [ER]

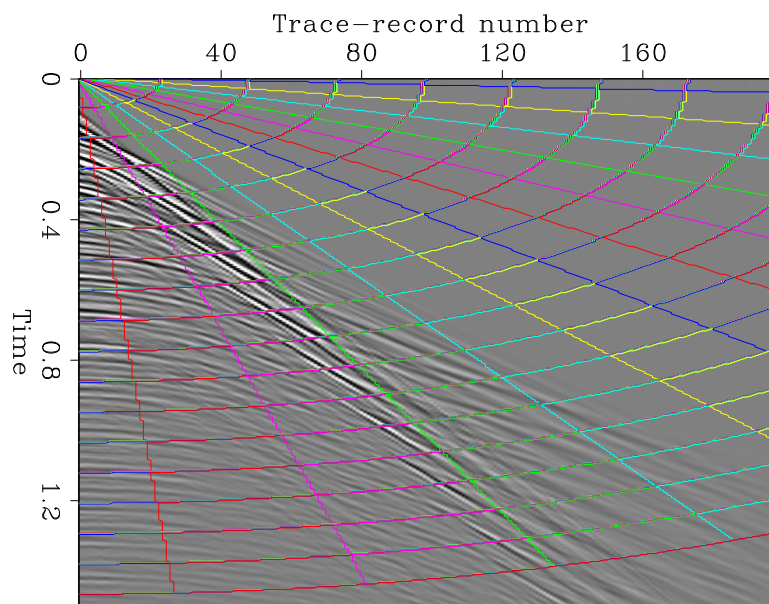


Figure 11: Example CMP gather overlaid by patch boundaries. Smoothing of filter coefficients is adjustable in r and θ . [bob3-web](#) [ER]

weak energy where the data was locally monodip. It is not clear that this happened.

ACKNOWLEDGMENTS

We thank Dave Nichols for encouraging discussions.

REFERENCES

- Abma, R., 1995, Least-squares separation of signal and noise with multidimensional filters: Ph.D. thesis, Stanford University.
- Bednar, J. B., 1997, Least squares dip and coherency attributes: *SEP-95*, 219–225.
- Canales, L. L., 1984, Random noise reduction: 54th Annual Internat. Mtg., Soc. Expl. Geophys., Expanded Abstracts, Session:S10.1.
- Claerbout, J. Fundamentals of Geophysical Data Processing: <http://sepwww.stanford.edu/sep/prof/>, 1976.
- Claerbout, J. F., 1978, Snell waves: *SEP-15*, 57–72.
- Claerbout, J. F., 1992a, Earth Soundings Analysis: Processing Versus Inversion: Blackwell Scientific Publications.
- Claerbout, J. F., 1992b, Earth Soundings Analysis: Processing versus Inversion: Blackwell Scientific Publications.
- Claerbout, J. F., 1992c, Information from smiles: Mono-plane-annihilator weighted regression: *SEP-73*, 409–420.
- Claerbout, J. F., 1992d, Nonstationarity and conjugacy: Utilities for data patch work: *SEP-73*, 391–400.
- Claerbout, J. F., 1995, Basic Earth Imaging: Stanford Exploration Project.
- Claerbout, J. F., 1997, Geophysical exploration mapping: Environmental soundings image enhancement: Stanford Exploration Project.
- Claerbout, J. Geophysical Estimation by Example: Environmental soundings image enhancement: <http://sepwww.stanford.edu/sep/prof/>, 1998.
- Claerbout, J., 1998b, Multidimensional recursive filters via a helix: *SEP-97*, 319–336.
- Claerbout, J. F., 1998c, Multi-dimensional recursive filtering via the helix: *Geophysics*, **63**, no. 5, 1532–1541.
- Clapp, R. G., Fomel, S., and Claerbout, J., 1997, Solution steering with space-variant filters: *SEP-95*, 27–42.

Crawley, S., Clapp, B., and Claerbout, J., 1998, Decon and interpolation with nonstationary filters: SEP-97, 183-192.

Crawley, S., 1998, Shot interpolation for radon multiple suppression: SEP-97, 173-182.

Crawley, S., 1999, Interpolation with smoothly nonstationary prediction-error filters: SEP-100, 181-196.

Fomel, S., Clapp, R., and Claerbout, J., 1997, Missing data interpolation by recursive filter preconditioning: SEP-95, 15-25.

Ottolini, R., 1982, Migration of reflection seismic data in angle midpoint coordinates: Ph.D. thesis, Stanford University.

Schwab, M., 1998, Enhancement of discontinuities in seismic 3-D images using a Java estimation library: Ph.D. thesis, Stanford University.

Soubaras, R., 1994, Signal-preserving random noise attenuation by the f-x projection: 64th Annual Internat. Mtg., Soc. Expl. Geophys., Expanded Abstracts, 1576-1579.

Spitz, S., 1991, Seismic trace interpolation in the f-x domain: Geophysics, 56, no. 6, 785-794.

Yilmaz, O., 1987, Seismic data processing: Soc. Expl. Geophys., Tulsa, OK.

